REFERENCES AND NOTES

1. G. W. Parshall and S. D. Ittel, *Homogeneous Catalysis* (Wiley, New York, ed. 2, 1992).
2. M. Grayson, Ed., *Kirk-Othmer Concise Encyclopedia of Chemical Technology* (Wiley, New York, 1985), pp. 505–518.
3. D. R. Fahey and J. E. Mahan, *J. Am. Chem. Soc.* **99**, 2501 (1977); M. T. Jones and R. N. McDonald, *Organometallics* **7**, 1221 (1988); C. J. Burns and R. A. Andersen, *J. Chem. Soc. Chem. Commun.* **1989**, 136 (1989); P. L. Watson, T. H. Tulip, I. Williams, *Organometallics* **9**, 1999 (1990); W. D. Jones, M. G. Partridge, R. N. Perutz, *J. Chem. Soc. Chem. Commun.* **1991**, 264 (1991); P. Hofmann and G. Unfried, *Chem. Ber.* **125**, 659 (1992); S. Hintermann, P. S. Pregosin, H. Rüegger, H. C. Clark, *J. Organomet. Chem.* **435**, 225 (1992); A. H. Klahn, M. H. Moore, R. N. Perutz, *J. Chem. Soc. Chem. Commun.* **1992**, 1699 (1992); R. G. Harrison and T. G. Richmond, *J. Am. Chem. Soc.* **115**, 5303 (1993); M. Weydert, R. A. Andersen, R. G. Bergman, *ibid.*, p. 8837.
4. S. T. Belt, M. Helliwell, W. D. Jones, M. G. Partridge, R. N. Perutz, *J. Am. Chem. Soc.* **115**, 1429 (1993).
5. O. Blum, F. Frolow, D. Milstein, *J. Chem. Soc. Chem. Commun.* **1991**, 258 (1991).
6. M. Aizenberg and D. Milstein, unpublished results. The x-ray structure of **1a** is not shown here. Abbreviations: Ph, phenyl; Me, methyl; Et, ethyl.
7. Supplementary material is available from the authors, including experimental procedures and characterization for complexes **1a**, **2**, and **3** and full x-ray structural data of complexes **2** and **3**.
8. For the mass spectrometry of Me_2PhSiF, see G. Dube and E. Gey, *Org. Mass Spectrom.* **14**, 17 (1979).
9. Prepared according to D. L. Thorn and R. L. Harlow, *Inorg. Chem.* **29**, 2017 (1990).
10. M. I. Bruce, B. L. Goodall, G. L. Sheppard, F. G. A. Stone, *J. Chem. Soc. Dalton Trans.* **1975**, 591 (1975); C. M. Anderson, R. J. Puddephatt, G. Ferguson, A. J. Lough, *J. Chem. Soc. Chem. Commun.* **1989**, 1297 (1989); A. D. Selmeczy, W. D. Jones, M. G. Partridge, R. N. Perutz, *Organometallics* **13**, 522 (1994).
11. M. Crespo, M. Martinez, J. J. Sales, *J. Chem. Soc. Chem. Commun.* **1992**, 822 (1992); *Organometallics* **12**, 4297 (1993); B. L. Lucht, M. J. Poss, M. A. King, T. G. Richmond, *J. Chem. Soc. Chem. Commun.* **1991**, 400 (1991).
12. R. Walsh, in *The Chemistry of Organic Silicon Compounds*, S. Patai and Z. Rappoport, Eds. (Wiley, New York, 1989), vol. 1, chap. 5.
13. M. Aizenberg and D. Milstein, *Angew. Chem. Int. Ed. Engl.* **33**, 317 (1994).
14. P. N. Rylander, *Catalytic Hydrogenation Over Platinum Metals* (Academic Press, New York, 1967), p. 424.
15. When C_6F_5D was used in reaction 7, only 1,4-C_6F_4HD was formed. Analysis of the recovered reactants revealed essentially no formation of C_6F_5H or of $(EtO)_3SiD$. Similarly, using $(EtO)_3SiD$ in reaction 7 resulted in exclusive formation of 1,4-C_6F_4HD. Analysis of recovered pentafluorobenzene revealed no exchange of H with D. This indicates a mechanism analogous to the one shown in Fig. 3 and excludes participation of a facile equilibrium

$$(EtO)_3SiRhL_3 + C_6F_5H \rightleftharpoons (EtO)_3SiH + C_6F_5RhL_3$$

16. Selected data for the reaction of **2**, $(EtO)_3SiH$, and C_6F_6 (1:120:450) are 94°C, 48 hours, and 38 turnovers for C_6F_5H; for the reaction of **2**, $(EtO)_3SiH$, and C_6F_5H (1:120:450), data are 94°C, 48 hours, and 33 turnovers for 1,4-$C_6F_4H_2$. The C_6F_6 and C_6F_5H used were rigorously checked for the presence of C_6F_5H and $C_6F_4H_2$, respectively, but none was found by ^1H and ^{19}F NMR. Control experiments (without **2** added) under the reaction conditions also did not yield these compounds.
17. W. E. Wentworth, T. Limero, E. C. M. Chen, *J. Phys. Chem.* **91**, 241 (1987).
18. B. E. Smart, in *The Chemistry of Functional Groups, Supplement D*, S. Patai and Z. Rappoport, Eds. (Wiley, New York, 1983), chap. 14.
19. Although the origin of regioselectivity is not clear, it is compatible with both electron transfer and nucleophilic oxidative addition. In both cases, the most polar C–F bond (the one para to H) is expected to be the most reactive.
20. C–F hydrogenolysis using heterogeneous catalysis was reported; reaction of polyfluorobenzenes is nonselective and requires very high temperatures [M. Hudlicky, *Chemistry of Organic Fluorine Compounds* (Prentice-Hall, New York, ed. 2, 1992), p. 175].
21. The drawing and data are given for one (of two) independent molecules of **3**.

22. We thank S. Cohen and F. Frolow for performing the x-ray crystallographic studies. Supported by the Basic Research Foundation, Jerusalem, Israel, and by the MINERVA Foundation, Munich, Germany. We are grateful to Hoechst, A-6, Frankfurt, Germany, for chemicals.

14 March 1994; accepted 1 June 1994

Probing Single Molecule Dynamics

X. Sunney Xie* and Robert C. Dunn

The room temperature dynamics of single sulforhodamine 101 molecules dispersed on a glass surface are investigated on two different time scales with near-field optics. On the 10^{-2}- to 10^2-second time scale, intensity fluctuations in the emission from single molecules are examined with polarization measurements, providing insight into their spectroscopic properties. On the nanosecond time scale, the fluorescence lifetimes of single molecules are measured, and their excited-state energy transfer to the aluminum coating of the near-field probe is characterized. A movie of the time-resolved emission demonstrates the feasibility of fluorescence lifetime imaging with single molecule sensitivity, picosecond temporal resolution, and a spatial resolving power beyond the diffraction limit.

Single molecule detection has recently been achieved at cryogenic temperatures (*1*, *2*), in liquids with flow cytometry (*3*), in aerosol particles (*4*) and electrophoresis gels (*5*), and at interfaces with near-field optics (6–9). These results offer exciting possibilities in many fields, including analytical chemistry, materials research, and the biological sciences. In particular, near-field microscopy (*10*) permits the fluorescence imaging of single chromophores in ambient environments with nanometer spatial resolution (6–9). Moreover, Betzig and Chichester have recently shown that this technique can not only locate the single chromophores but also determine their orientations (6). Time-resolved spectroscopy combined with near-field optics (*11*, *12*) will allow one to probe dynamical processes such as molecular motions and chemical reactions on a single molecule basis.

In near-field microscopy, sub–diffraction-limited spatial resolution is achieved by bringing a subwavelength spot of light close to a sample such that the resolution is only limited by the size of the spot. Single molecule sensitivity results from the high photon flux delivered by the tapered single mode fiber probe (*13*), efficient background rejection resulting from the small illumination area, and possibly, excitation by strong evanescent wave components near the tip end (*14*). The sides of the tapered near-field probe are coated with about 90 nm of aluminum to prevent light leakage, with an aperture of about 100 nm capable of delivering 10^{10} photons per second. A feedback mechanism based on shear force, similar to that previously reported (*15*, *16*), is implemented to regulate the tip-sample gap with a vertical resolution of better than 1 nm. The total emission is collected from beneath a transparent sample by a detection

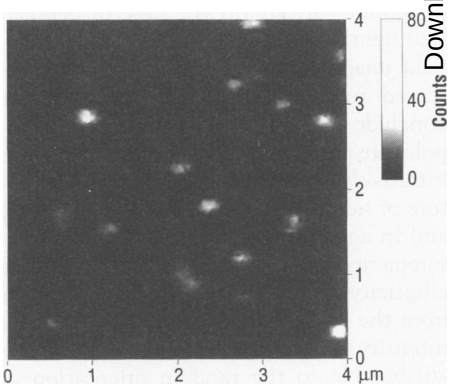

Fig. 1. Near-field fluorescence image of sulforhodamine 101 molecules dispersed on a glass surface. The bright features in the 4 μm by 4 μm (256 pixels by 256 pixels, 8-ms averaging time per pixel) image result from emission from single molecules. Linearly polarized excitation light aligned with the *x* axis was used. The FWHM of the sub–diffraction-limited features are 125 nm, which corresponds to the aperture diameter of the tip used in the imaging.

Pacific Northwest Laboratory, Molecular Science Research Center, P.O. Box 999, Richland, WA 99352, USA.

*To whom correspondence should be addressed.

system designed to maximize the collection efficiency and background rejection, which are necessary for single molecule sensitivity (*17, 18*). The sample is raster scanned with a closed-loop *xy* scanner (Queensgate) containing capacitance-based sensors (positioning accuracy of better than 1 nm), which avoids complications associated with piezo hysteresis. This feature allows us to quickly and accurately position the tip above a molecule.

Figure 1 shows a 4 μm by 4 μm near-field emission image of sulforhodamine 101 molecules dispersed on a glass cover slip. The bright, sub–diffraction-limited spots observed are attributable to emission from single molecules and exhibit a full width at half maximum (FWHM) of 125 nm, limited by the aperture size of the particular near-field probe used. The sudden and permanent disappearance of some of these features in subsequent images as a result of irreversible photochemical reactions is indicative of single molecules.

The excitation polarization used in collecting Fig. 1 was linearly polarized along the *x* (horizontal) axis with an extinction ratio of 80:1 when viewed in the far field. The electric field distribution in the near field of a subwavelength aperture in a conducting screen has been calculated (*20, 21*) and qualitatively confirmed experimentally (*6*). Accordingly, the electric field component along the *y* direction should be significantly smaller than that along the *x* direction in our experimental arrangement. There is, however, a strong electric field component along the *z* direction at the edges of the near-field aperture. For molecules with transition dipoles projected into the *z* direction, a crescent-shaped pattern (for linearly polarized excitation) or a doughnut pattern (in the case of depolarized light) should be expected in the near-field image (*6*). Those shapes are not observed in Fig. 1, and we can therefore conclude that the molecular transition dipoles are parallel to the glass surface. This is intuitively consistent with the planar structure of sulforhodamine 101 (Fig. 2C, inset) and in agreement with previous bulk measurements on the same system (*22*). The ellipticity of the features in Fig. 1 results from the polarized excitation (*6*), and the intensity variation between the molecules is attributable to the random orientation of the molecular dipoles on the surface plane or differences in their absorption spectra.

Successive scans of the same area revealed intensity changes and even the sudden appearance of bright new features, similar to observations made in a related system (*7*). To understand this behavior, we positioned the tip above a molecule and recorded the emission counts as a function of time (Fig. 2A). Sudden jumps indicative of single molecule dynamics are observed in the emission signal until it finally drops to the background level as the molecule is photobleached. One possible mechanism for the jumps involves molecular reorientation on the surface (*7*).

To investigate this phenomena, we modulated the polarization of the excitation light between the *x* and *y* directions with a Pockels' cell (Fig. 2B). Throughout the course of the experiment, a constant signal close to the background level was observed for the *y*-polarized excitation. For *x*-polarized excitation, however, there were sudden fluctuations in the emission signal, clearly beyond the noise level, similar to those observed in Fig. 2A. This observation rules out the possibility of molecular reorientation as the origin of the abrupt emission jumps.

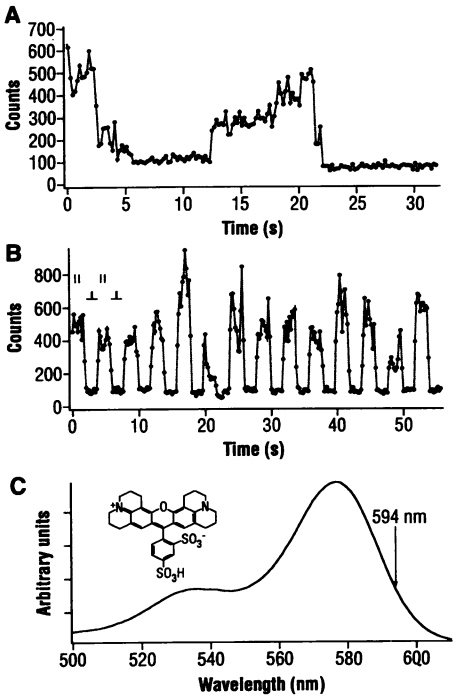

Fig. 2. (**A**) Emission counts as a function of time (0.2-s bins) collected by centering the near-field probe directly above a single molecule. Sudden jumps are observed before the photobleaching of the molecule. (**B**) With the tip positioned above another molecule, the excitation polarization was modulated (0.25 Hz) between *x* and *y* polarizations with a Pockels' cell. The transition dipole of this molecule is oriented along the *x* direction, resulting in a large modulation. A constant signal close to the background level is observed for the *y*-polarized excitation, and there are sudden fluctuations in the emission signal derived from *x*-polarized excitation. This indicates that molecular reorientation is not the cause of the sudden jumps in emission observed in (A). (**C**) Excitation spectrum of 200 nM solution of sulforhodamine 101 in methanol. For (A) and (B), the molecules were excited at 594 nm, and the total emission was detected. (**Inset**) The molecular structure of sulforhodamine 101.

We attribute the observed behavior to spectral diffusion of the molecules. Single molecule spectral diffusion has been observed in excitation spectra taken at liquid helium temperature (*23*). Recently, changes of single molecule emission spectra with time have been seen on polymethylmethacrylate films at room temperature with near-field optics (*8*). The fluctuations in the emission intensity observed in the present study may result from variations in the absorption cross section at the excitation wavelength, caused by changes in the single molecule absorption spectrum. The spectral diffusion can result from thermal fluctuations of the molecule and its environment or from a photoinduced molecular process (for example, conformational changes or perturbations induced by excess energy released in nonradiative relaxation). Although a detailed study is needed to address these issues and their implications to the spectral lineshape, these observations reveal molecular-level dynamics that are present in absorption and fluorescence measurements but are otherwise hidden in experiments conducted on large ensembles of molecules.

To investigate the picosecond dynamics of a single molecule, we coupled a 10-MHz train of ultrashort light pulses (5-ps FWHM, 594 nm, bandwidth < 1 nm, 300-μW average power) from a cavity-dumped, synchronously pumped dye laser (Coherent 702) to the near-field probe. We have recently demonstrated fluorescent lifetime measurements using time-correlated photon counting coupled with near-field optics by studying the fluorescence lifetime of intact photosynthetic membranes (*11*).

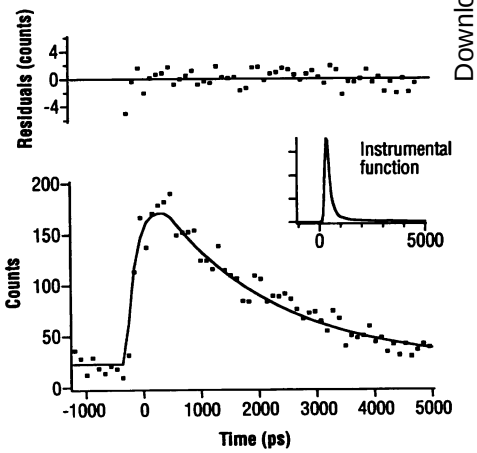

Fig. 3. Time-resolved fluorescence decay of a single sulforhodamine 101 molecule on a glass surface, taken by placing the near-field probe directly above the molecule. The decay is fit (solid line) with a single exponential convoluted with (**inset**) the instrument response function (FWHM, 250 ps). The weighted residuals are shown above (chi square = 1.2). The measured lifetime is 2.0 ± 0.25 ns.

The single molecule fluorescence decay (Fig. 3) was measured by placing the center of the fiber tip 7 nm above one of the sulforhodamine 101 molecules in Fig. 1. The data were fit (solid line) with a single exponential decay of 2.0 ns convoluted with the instrumental response function (Fig. 3, inset). This lifetime is compared with that previously reported (2.7 ns) for a submonolayer coverage of sulforhodamine 101 molecules absorbed on borosilicate glass surfaces (*22*). The reason for the shorter lifetime measured is discussed below.

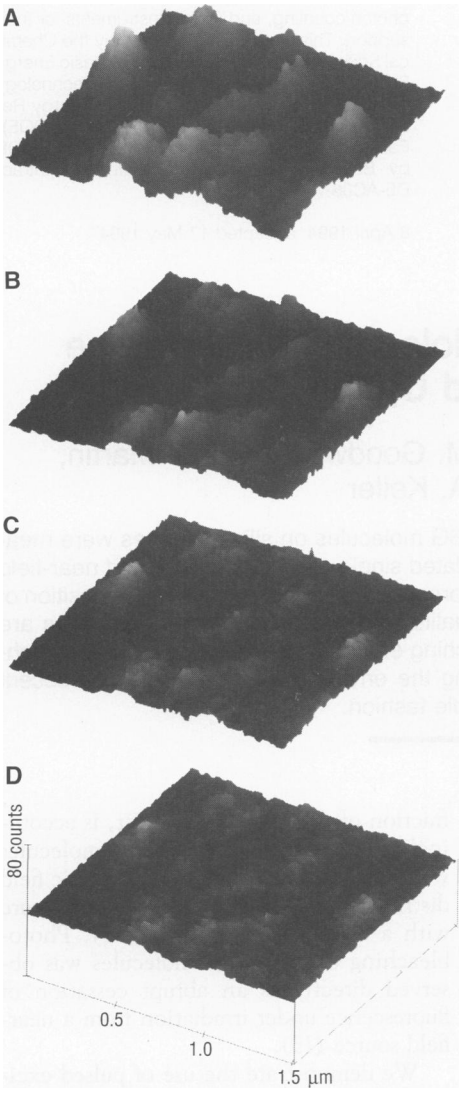

Fig. 4. Time-resolved near-field fluorescence images (1.5 μm by 1.5 μm) of single sulforhodamine 101 dye molecules dispersed on a glass surface at time delays of (**A**) 0 ns, (**B**) 1.5 ns, (**C**) 3.0 ns, and (**D**) 4.5 ns after excitation with picosecond light pulses. These four images were extracted from a movie of 64 frames (2 μm by 2 μm) spanning a total of 6.6 ns. This movie, collected in 20 min, contains a vast amount (2 megabytes in binary form) of spatial and temporal information demonstrating the feasibility of lifetime imaging with single molecule sensitivity, picosecond time resolution, and a spatial resolving power beyond the diffraction limit.

Fluorescence lifetime measurements on single fluorophores have been demonstrated at cryogenic temperatures (*24*) and at ambient temperatures in flow cytometry experiments (*25*). The near-field experiment reported here combines this high temporal resolution with high spatial resolution, which is particularly desirable for many biological applications. The fluorescence lifetime measures an intrinsic property of the molecular species and its particular environment, such as pH, the presence of quenchers, or binding to a protein or DNA. In recent years, fluorescence lifetime imaging with the use of confocal microscopy has undergone rapid advancements (*26, 27*). Below we demonstrate the feasibility of picosecond lifetime imaging with sub–diffraction-limit spatial resolution and single molecule sensitivity for two-dimensional samples.

For near-field fluorescence lifetime imaging, a three-dimensional histogram of emission counts (x,y,t) is collected as the sample is scanned (line scan rate of 0.5 Hz). A large, fast memory is configured such that 64 images (128 pixels by 128 pixels) are simultaneously accumulated, each corresponding to a different time delay between the excitation pulse and the emission photon. With this scheme, a movie spanning 6.6 ns was collected of the fluorescence decays of single sulforhodamine 101 molecules dispersed on a glass surface (Fig. 4).

The large amount of data contained in the movie enables us to characterize the quenching of the fluorescence by the aluminum coating of the near-field probe. This has been an unsolved technical issue in the development of near-field fluorescence microscopy. Not surprisingly, the fluorescence decays are dependent on the relative position between the tip and the molecules. Plots of the fluorescence lifetimes as a function of position across a molecule in the x direction (Fig. 5) show that when the tip is centered above the single molecule, the fluorescence lifetime is the longest (2.0 ns). As the tip is moved off center, excited-state energy transfer from the molecule to the aluminum coating substantially reduces the lifetime and, therefore, the fluorescence quantum yield. Similar behavior is seen in the y direction.

The radiative and nonradiative dynamics of molecules in front of mirrored surfaces have been extensively studied (*28–31*). When the fluorophore-mirror distance is on the order of the emission wavelength, the radiative rate oscillates with distance as a result of the interference of the emitted and reflected wave. When the distance is less than 10 nm, nonradiative energy transfer to the metal occurs with a strong distance dependence [d^{-3} or d^{-4}, depending on the mechanism (*30*)]. In a recent experiment with a submonolayer of Rhodamine 6G in front of an aluminum mirror, both spectral changes (2-nm gap) and substantially shortened fluorescence lifetimes (<6-nm gap) were observed (*31*). Fortunately, the tip-sample gap (>5 nm) in the near-field experiments and the specific geometry of the aluminum coating (Fig. 5) results in a weaker molecule-metal interaction. It is encouraging that our results indicate that the nonradiative energy transfer can be minimized when the tip is centered above the molecule. Further studies are under way to determine the tip-sample gap dependence in lifetime and the relative contributions of nonradiative and radiative rates. Fluorescence quenching should also be dependent on the orientation of the transition dipole with respect to the metal surface (*28*). The single molecule measurements shown above were performed on molecules with transition dipoles oriented parallel to the glass surface. The effect of spectral diffusion on the measured lifetime has not been evaluated.

From a practical point of view, quenching by the aluminum coating around the aperture actually enhances the spatial resolution in near-field fluorescence imaging. On the other hand, in order to avoid the complications of quenching on lifetime measurements, it is important to center the tip above the molecule. However, for sub-nanosecond dynamical processes, the fluorescence lifetimes should not be affected.

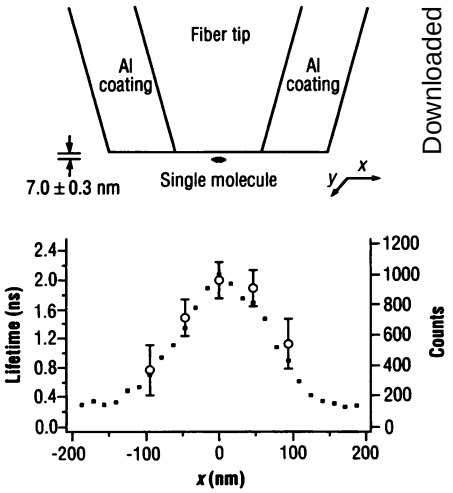

Fig. 5. Plot of the lifetime (open circles) and intensity (dots) (FWHM, 125 nm) as a function of x distance across the emission feature of a single molecule, extracted from the movie shown in Fig. 4. Above is a schematic of the near-field probe with its dimensions drawn on scale with the plot below. There is a substantial decrease in the fluorescence lifetime of the molecule near the sides of the fiber tip because of the quenching by the aluminum coating.

For longer processes and fluorescent objects comparable to or bigger than the tip, quenching can be further avoided by conducting measurements under liquid, where the frictional forces associated with the shear-force feedback mechanism allow for larger tip-sample separations (9). The fact that time-resolved fluorescence measurements on single chromophores can be performed in a nonpurtabative manner opens the way toward the study of chemical reactions on a single-molecule basis. Detailed studies of dynamical processes—such as photoinduced electron transfer, proton transfer, isomerization, or protein conformational changes—in specific local environments with known molecular orientations are now experimentally feasible.

REFERENCES AND NOTES

1. W. E. Moerner and L. Kador, *Phys. Rev. Lett.* **62**, 2535 (1989).
2. M. Oritt and J. Bernard, *ibid.* **65**, 2716 (1990).
3. E. B. Shera, N. K. Seitzinger, L. M. Davis, R. A. Keller, S. A. Soper, *Chem. Phys. Lett.* **174**, 553 (1990).
4. M. D. Barnes, K. C. Nig, W. B. Whitten, J. M. Ramsey, *Anal. Chem.* **65**, 2360 (1993).
5. A. Castro and B. Shera, in *Laser Applications to Chemical Analysis*, vol. 5 of *Technical Digest Series* (Optical Society of America, Washington, DC, 1994), p. 210.
6. E. Betzig and R. J. Chichester, *Science* **262**, 1422 (1993).
7. W. P. Ambrose, P. M. Goodwin, J. C. Martin, R. A. Keller, *Phys. Rev. Lett.* **72**, 132 (1994).
8. J. K. Trautman, J. J. Macklin, L. E. Brus, E. Betzig, *Nature* **369**, 40 (1994).
9. X. S. Xie, E. V. Allen, G. R. Holtom, R. C. Dunn, L. Mets, in *Proc. SPIE* **2137**, 264 (1994).
10. E. Betzig and J. K. Trautman, *Science* **257**, 189 (1992); D. W. Pohl, in *Advances in Optical and Electron Microscopy*, T. Mulvey and C. J. R. Sheppard, Eds. (Academic Press, New York, 1991), vol. 12, pp. 243–312.
11. R. C. Dunn, G. R. Holtom, L. Mets, X. S. Xie, *J. Phys. Chem.* **98**, 3094 (1994).
12. W. P. Ambrose, P. M. Goodwin, J. C. Martin, R. A. Keller, *Proc. SPIE* **2125**, 2 (1994).
13. E. Betzig, J. K. Trautman, T. D. Harris, J. S. Weiner, R. L. Kostelak, *Science* **251**, 1468 (1991).
14. U. Durig, D. W. Pohl, F. Rohner, *J. Appl. Phys.* **59**, 3318 (1986).
15. E. Betzig, P. L. Finn, J. S. Weiner, *Appl. Phys. Lett.* **60**, 2484 (1992).
16. R. Toledo-Crow, P. C. Yang, Y. Chen, M. Vaez-Iravani, *ibid.*, p. 2957.
17. R. C. Dunn, E. V. Allen, S. A. Joyce, G. A. Anderson, X. S. Xie, *Ultramicroscopy*, in press.
18. The tip feedback and *xy* scanner are interfaced with a Nanoscope III controller (Digital Instruments). The near-field assembly and sample stage are built onto an inverted fluorescence microscope (Nikon Diaphot). The optics train is as follows: linearly polarized 594-nm HeNe laser (Particle Measuring Sytems, bandwidth <1 GHz); optical shutter; acousto-optic intensity stabilizer (LiCONix), holographic bandpass prism (Kaiser Optical Systems); variable neutral density filter (Reynard); λ/2 and λ/4 plates (Newport); fiber coupler (Newport, ×20 objective lens); 2 m of single mode fiber (Corning Flexcore 633) with the near-field probe at the end; transparent sample; oil immersion objective lens (Nikon, ×100, numerical aperture 1.3); holographic beam splitter and holographic notch plus filter for 594 nm (Kaiser Optical Systems); optics inside the inverted fluorescence microscope directing the emission to the output port; dielectric filter (Corion LS-950.S.1166F, for rejection of scattered 1.15-μm light from a HeNe laser used for shear-force feedback); 3-cm focal lens; and an avalanche photodiode detector [EG&G Canada, #SPCM-200 modified for fast time response (*19*)]. The sample was prepared by dispersing a dilute methanol solution of sulforhodamine 101 (Exciton) (2×10^{-9} M) on a borosilicate glass cover slip (Becton Dickinson, no. 3305). All experiments were performed on dry sample at room temperature.
19. L. Li and L. M. Davis, *Rev. Sci. Instrum.* **64**, 1524 (1993).
20. H. A. Bethe, *Phys. Rev.* **66**, 163 (1944).
21. C. J. Bouwkamp, *Philips Res. Rep.* **5**, 321 (1950); *ibid.*, p. 401.
22. M. Lieberherr, C. Fattinger, W. Lukosz, *Surf. Sci.* **189**, 954 (1987).
23. W. P. Ambrose and W. E. Moerner, *Nature* **349**, 225 (1991); W. E. Moerner and T. Basche, *Angew. Chem.* **32**, 457 (1993); P. T. Tchenio, A. B. Myers, W. E. Moerner, *J. Lumin.* **56**, 1 (1993).
24. M. Pirotta *et al.*, *Chem. Phys. Lett.* **208**, 379 (1993).
25. S. A. Soper, L. M. Davis, E. B. Shera, *J. Opt. Soc. Am. B.* **9**, 1761 (1992).
26. J. A. Lakowicz, H. Szmacinski, K. Nowaczyk, M. L. Johnson, *Proc. Natl. Acad. Sci. U.S.A.* **89**, 1271 (1992).
27. X. F. Wang, A. Periasamy, B. Herman, D. M. Coleman, *Crit. Rev. Anal. Chem.* **23**, 369 (1992).
28. R. R. Chance, A. Prock, R. Silbey, *Adv. Chem. Phys.* **37**, 1 (1978).
29. K. H. Drexahage, in *Progress in Optics XII*, E. Wolf, Ed., (North-Holland, New York, 1974), p. 165.
30. P. Avouris and B. N. J. Persson, *J. Phys. Chem.* **88**, 837 (1984); B. N. J. Persson and N. D. Lang, *Phys. Rev. B* **26**, 5409 (1982); B. N. J. Persson and M. Persson, *Surf. Sci.* **97**, 609 (1980); B. N. J. Persson, *J. Phys. C* **11**, 4251 (1978).
31. G. Cnossen, K. E. Drabe, D. A. Wiersma, *J. Chem. Phys.* **98**, 5276 (1993).

32. We thank G. Anderson for designing the multidimensional histogram electronics, E. Vey Allen for his assistance in the development of the microscope, S. D. Colson for stimulating discussions, G. Holtom for assistance with time-correlated photon counting, and Digital Instruments for their support. This work was supported by the Chemical Sciences Division of the Office of Basic Energy Sciences and in part by Laboratory Technology Transfer Program within the Office of Energy Research of the U.S. Department of Energy (DOE). Pacific Northwest Laboratory is operated for DOE by Battelle Memorial Institute under contract DE-AC06-76RLO 1830.

8 April 1994; accepted 17 May 1994

Alterations of Single Molecule Fluorescence Lifetimes in Near-Field Optical Microscopy

W. Patrick Ambrose,* Peter M. Goodwin, John C. Martin, Richard A. Keller

Fluorescence lifetimes of single Rhodamine 6G molecules on silica surfaces were measured with pulsed laser excitation, time-correlated single photon counting, and near-field scanning optical microscopy (NSOM). The fluorescence lifetime varies with the position of a molecule relative to a near-field probe. Qualitative features of lifetime decreases are consistent with molecular excited state quenching effects near metal surfaces. The technique of NSOM provides a means of altering the environment of a single fluorescent molecule and its decay kinetics in a repeatable fashion.

Experiments on single molecules reveal details of molecular environments that are indiscernible in bulk measurements. Optical single molecule detection has been reported in liquids (*1–6*), in solids (*7–11*), and on surfaces (*12–16*), where single molecules are used as probes of individual local environments and as indicators of unimolecular events. The technique used to detect single molecules on surfaces under ambient conditions, NSOM, is a scanned probe microscopy that uses a subwavelength optical aperture to illuminate a subdiffraction limited area on a surface (*17*). In NSOM, small areas are illuminated with high irradiance and low power. Single molecule sensitivity is attained because the background scattered light, which is a fixed fraction of the excitation power, is accordingly low. Single fluorescent molecules were used to probe the optical electric field distribution around a near-field aperture with a diameter of ~50 nm (*12*). Photobleaching of individual molecules was observed directly as an abrupt cessation of fluorescence under irradiation from a near-field source (*13*).

We demonstrate the use of pulsed excitation and time-correlated single photon counting (TCSPC) to resolve temporally the fluorescence from individual Rhodamine 6G (R6G) molecules on silica located <10 nm from an NSOM probe. In TCSPC, the elapsed time between an excitation pulse and a detected photon is measured. A histogram of the elapsed times provides a fluorescence decay curve, from which the fluorescence lifetime (τ) is extracted. As a single R6G molecule is moved near an NSOM probe, τ varies repeatably with position under the probe. Qualitative features of some alterations in τ are consistent with

W. P. Ambrose, P. M. Goodwin, R. A. Keller, Chemical Science and Technology Division, Los Alamos National Laboratory, Los Alamos, NM 87545, USA.
J. C. Martin, Life Sciences Division, Los Alamos National Laboratory, Los Alamos, NM 87545, USA.

*To whom correspondence should be addressed.